Distributed measurement of high electric current by means of polarimetric optical fiber sensor

Luca Palmieri,[1,*] **Davide Sarchi,**[2] **and Andrea Galtarossa**[1,3]

[1]*Department of Information Engineering, University of Padova, Via G. Gradenigo 6/B, 35131 Padova, Italy*
[2]*Prysmian S.p.A., V.le Sarca 222, Milano, Italy*
[3]*International Institute for Urban Systems Engineering, Southeast University, Nanjing, China*
[*]*luca.palmieri@dei.unipd.it*

Abstract: A novel distributed optical fiber sensor for spatially resolved monitoring of high direct electric current is proposed and analyzed. The sensor exploits Faraday rotation and is based on the polarization analysis of the Rayleigh backscattered light. Preliminary laboratory tests, performed on a section of electric cable for currents up to 2.5 kA, have confirmed the viability of the method.

OCIS codes: (060.2270) Fiber characterization; (060.2300) Fiber measurements.

References

1. K. T. V. Grattam, B. T. Maggitt, *Optical Fiber Sensor Technology* (Kluwer Academic Publishers, 2000).
2. S. C. Rashleigh and R. Ulrich, "Magneto-optic current sensing with birefringent fibers," Appl. Phys. Lett. **34**, 768–770 (1979).
3. S. C. Rashleigh, "Magnetic-field sensing with a single-mode fiber," Opt. Lett. **6**, 19–21 (1981).
4. R. Laming and D. Payne, "Electric current sensors employing spun highly birefringent optical fibers," J. Lightwave Technol. **7**, 2084 –2094 (1989).
5. V. Annovazzi-Lodi, S. Donati, and S. Merlo, "Coiled-fiber sensor for vectorial measurement of magnetic field," J. Lightwave Technol. **10**, 2006–2010 (1992).
6. K. Bohnert, P. Gabus, J. Kostovic, and H. Brändle, "Optical fiber sensors for the electric power industry," Opt. Laser Eng. **43**, 511–526 (2005).
7. A. J. Rogers, "Polarization-optical time domain reflectometry: a technique for the measurement of field distributions," Appl. Opt. **20**, 1060–1074 (1981).
8. J. N. Ross, "Measurement of magnetic field by polarisation optical time-domain reflectometry," Electron. Lett. **17**, 596–597 (1981).
9. L. Palmieri and A. Galtarossa, "Distributed polarization-sensitive reflectometry in nonreciprocal single-mode optical fibers," J. Lightwave Technol. **29**, 3178–3184 (2011).
10. L. Palmieri and A. Galtarossa, "Distributed fiber optic sensor for mapping of intense magnetic fields based on polarization sensitive reflectometry," Proc. SPIE **8351**, 835131 (2012).
11. M. Aerssens, A. Gusarov, P. Moreau, P. Malard, V. Massaut, P. Mégret, and M. Wuilpart, "Development of a Jones vector based model for the measurement of a plasma current in a thermonuclear fusion reactor with a POTDR setup," Proc. SPIE **8439**, 84390D (2012).
12. A. Masoudi and T. P. Newson, "Distributed optical fiber dynamic magnetic field sensor based on magnetostriction," Appl. Opt. **53**, 2833–2838 (2014).
13. L. Palmieri, "Distributed polarimetric measurements for optical fiber sensing," Optic. Fiber Technol. **19**, 720–728 (2013).
14. L. Palmieri, D. Sarchi, and A. Galtarossa, "Polarization optical fiber sensor for distributed current monitoring," Proc. SPIE **9157**, 91570O (2014).
15. R. Ulrich and A. Simon, "Polarization optics of twisted single-mode fibers," Appl. Opt. **18**, 2241–2251 (1979).
16. J. Noda, T. Hosaka, Y. Sasaki, and R. Ulrich, "Dispersion of verdet constant in stress-birefringent silica fibre," Electron. Lett. **20**, 906–908 (1984).

#232204 - $15.00 USD Received 14 Jan 2015; revised 10 Mar 2015; accepted 12 Mar 2015; published 21 Apr 2015

17. R. Jopson, L. Nelson, and H. Kogelnik, "Measurement of second-order polarization-mode dispersion vectors in optical fibers," IEEE Photon. Technol. Lett. **11**, 1153 –1155 (1999).
18. K. Kanatani, "Analysis of 3-d rotation fitting," IEEE Trans. Pattern Anal. Mach. Intell. **16**, 543–549 (1994).
19. L. Palmieri, T. Geisler, and A. Galtarossa, "Limits of applicability of polarization sensitive reflectometry," Opt. Express **19**, 10874–10879 (2011).
20. S. C. Rashleigh and R. Ulrich, "High birefringence in tension-coiled single-mode fibers," Opt. Lett. **5**, 354–356 (1980).
21. L. Palmieri, "Accurate distributed characterization of polarization properties in optical fibers," in *36th European Conference on Optical Communications,* (IEEE, 2010), pp. 1–6.
22. A. Galtarossa and L. Palmieri, "Measure of twist-induced circular birefringence in long single-mode fibers: theory and experiments," J. Lightwave Technol. **20**, 1149–1159 (2002).
23. S. M. Kay, *Modern Spectral Estimation* (Prentice-Hall, 1988).

1. Introduction

Among the several advantages offered by optical fiber sensors (OFSs), the possibility of performing distributed monitoring of various physical fields is the most unique. Distributed sensing by optical fiber is achieved by analyzing in a proper way the light generated by one of the scattering processes that may take place in a fiber, namely: Rayleigh, Brillouin and Raman scattering [1]. Distributed sensors of temperature and strain based on these phenomena are nowadays commercial products.

Magnetic field sensors based on optical fibers are among the earliest example of OFSs [2–6], and have found commercial application in the measurement of electric current. With the exception of few very preliminary experiments [7, 8], distributed magnetic field sensors have been proposed only recently [9–12], and their application to distributed current measurement is still largely unexplored. Masoudi and Newson [12] have reported a distributed magnetic field OFS in which the fiber is coupled to a nickel wire that transduces magnetic field strength in strain. The sensor can potentially cover kilometer-range distances with spatial resolution of 1 m, but it has been tested only over a length of 8 m, as it requires the implementation of a very specific cable structure. However, good sensitivity of 0.1 mT and wide bandwidth from 50 Hz to 5000 Hz have been reported.

An alternative approach to distributed magnetic field OFS consists in exploiting Faraday rotation of polarization [7–11]. In this case, polarization sensitive reflectometry is used to measure the state of polarization (SOP) of Rayleigh backscattered light [13], from which amplitude and sign of the magnetic field component parallel to the fiber axis can be retrieved with proper data analysis. Preliminary applications have shown that, although limited to static fields over distances of some tens of meters and with sensitivity of about 100 mT, this technique can be successfully used to measure vector maps of intense magnetic field in the area spanned by the fiber, with spatial resolution of few centimeters and using standard telecommunication fibers [10, 13].

In this paper we discuss the application of the above polarimetric method to the distributed measurement of electric current. Experimental tests, preliminarily reported in [14], confirm the viability of the approach. Direct currents up to 2.5 kA have been successfully measured along an 80-m-long electric circuit (corresponding to 240 m of optical fiber), with 4 m of spatial resolution (in terms of electrical cable length) and about 100 A of current resolution. To the best of our knowledge this is the first time that a distributed optical fiber current sensor is described.

2. Measurement principle

The sensor basically consists of a fiber helically wound around the conducting wire (hereinafter assumed straight), with radius R and pitch p [see Fig. 1(b)]. By Biot-Savart law the magnetic induction field generated by the conductor is oriented along the azimuthal coordinate and has nominal amplitude $B = \mu_0 I/(2\pi r)$, where I is the flowing direct current, r is the radial distance

#232204 - $15.00 USD Received 14 Jan 2015; revised 10 Mar 2015; accepted 12 Mar 2015; published 21 Apr 2015

from the conductor axis and $\mu_0 = 4\pi \times 10^{-7}$ N/A^2. As a consequence of Faraday rotation, the SOP of light propagating in the fiber undergoes a rotation whose amplitude per unit length, in the 3-dimensional space of unit Stokes vectors, reads [15]

$$\eta(z) = 2VB(z)\cos\psi(z)\,, \tag{1}$$

where z is the longitudinal coordinate along the fiber, V the Verdet constant, $B(z)$ the intensity of the magnetic induction, and $\psi(z)$ the angle subtended by the magnetic induction and the fiber axis in the direction of forward propagation of light. For germano-silica optical fibers the Verdet constant expressed in rad/T/m is about $1.43/\lambda_{\mu m}^2$, where $\lambda_{\mu m}$ is the wavelength expressed in μm [16]; so, for example, at 1.55 μm we have $V \simeq 0.6$ rad/T/m.

When the fiber is helically wound as in the case at hand, $\cos\psi = 2\pi R/\ell$ where $\ell = [p^2 + (2\pi R)^2]^{1/2}$ is the length of a single fiber loop, and consequently $\eta(z) = 2\mu_0 V I/\ell$. It is interesting to observe that the Faraday rotation accumulated along a given fiber length is proportional to the number of fiber loops, independently of winding pitch and radius. Notice also that since the relationship between the length along the cable, z_e, and the length along the fiber, z, is $z_e = (p/\ell)z$, the Faraday rotation per unit length of electric cable is $\eta_e = 2\mu_0 V I/p$. Accordingly, the shorter the winding pitch the higher the sensor sensitivity; however, the shorter the pitch the longer the fiber needed to cover a given length of electric cable.

Before describing the experiment it is worthwhile briefly recalling the measurement principle. When a polarized optical pulse is sent in an optical fiber, the SOP of the light backscattered by Rayleigh scattering varies as a function of the scattering position z according to the equation $d\hat{s}_B/dz = \bar{\beta}_B(z) \times \hat{s}_B(z)$, where $\hat{s}_B(z)$ is the 3-dimensional Stokes unit vector representing SOP and $\bar{\beta}_B(z)$ is the so called round-trip birefringence vector [9]. It can be shown that in a proper reference frame $\bar{\beta}_B(z) = 2\mathbf{B}(z)\bar{\beta}(z)$, where the 3×3 Mueller matrix $\mathbf{B}(z)$ represents backward propagation from z to the fiber input, and $\bar{\beta}(z)$ is the local birefringence vector. Owing to the particular reference frame being used, the first two components of $\bar{\beta}(z)$ depend just on reciprocal polarization effects occurring at z, which include both linear birefringence (bending, anisotropy, lateral stress, etc.) and twist induced circular birefringence (optical activity). Quite differently, the third component $\beta_3(z)$ of $\bar{\beta}(z)$ depends only on nonreciprocal polarization effects, namely Faraday rotation, and in fact $\beta_3(z) = \eta(z)$ [9].

Hence both $\hat{s}_B(z)$ and $\bar{\beta}_B(z)$ encodes information about Faraday rotation. None of them, however, is a local quantity, for both depend on every polarization effect (not only Faraday rotation but also bending, twist, etc.) that occurs along the fiber, from its input to the scattering point z and back. Local information is encoded in $\bar{\beta}(z)$, but to calculate it from $\bar{\beta}_B(z)$ we need to determine the matrix $\mathbf{B}(z)$; however, it can be shown [9] that $\mathbf{B}(z)$ obeys the differential equation $d\mathbf{B}/dz = (1/2)\bar{\beta}_B(z) \times \mathbf{B}(z)$, with $\mathbf{B}(0) = \mathbf{I}$. Therefore we first have to measure $\hat{s}_B(z)$ for at least two different input SOPs; as described in [17] these do not need to be known, it is sufficient that they are different. From the measured $\hat{s}_B(z)$ the round-trip birefringence vector $\bar{\beta}_B(z)$ can be calculated with well known procedures [17,18]. Afterwards the matrix $\mathbf{B}(z)$ can be determined by numerically solving the above differential equation and, finally, the birefringence vector can be calculated as $\bar{\beta}(z) = (1/2)\mathbf{B}^T(z)\bar{\beta}_B(z)$ [9]. In this way local Faraday rotation is disentangled from all the other polarization effects.

3. Experimental layout and results

The measurement of $\hat{s}_B(z)$ can be performed in the time domain using a polarization OTDR, or in the frequency domain with a polarization OFDR (POFDR). In our experiments we opted for the POFDR, for it provides higher spatial resolution (few centimeters or below) and lower uncertainty in the measurement of the SOP (lower than 1%), albeit this comes at the cost of a reduced measurement range (shorter than 2 km). Its schematic is shown in Fig. 1(a); it consists

#232204 - $15.00 USD Received 14 Jan 2015; revised 10 Mar 2015; accepted 12 Mar 2015; published 21 Apr 2015

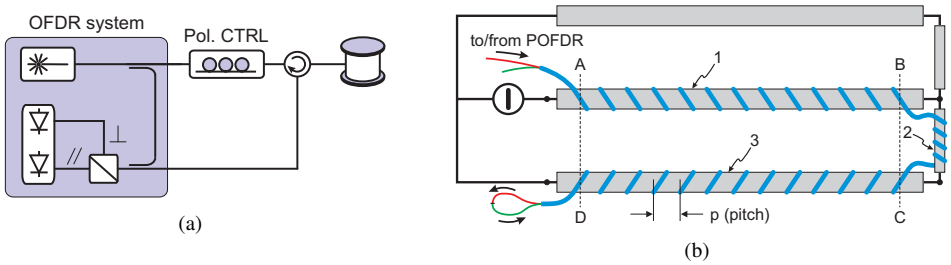

Fig. 1. (a) Schematic of the POFDR. (b) Schematic of the experimental layout; the loose tube helically wound around conductors No. 1, 2 and 3 contains several G.652 fibers, two of which are concatenated (drawing not in scale).

of a standard OFDR (scanning range: 5 nm; output power: 3 dBm) with a polarization controller in the source path, used to change the input SOP. Polarization analysis of the backscattered light is obtained by exploiting the polarization diversity coherent receiver, which measures amplitude and phase of each polarization components. Measurements take about 2 s for each input SOP, therefore the technique can be used only in static or quasi-static conditions.

The experimental layout is shown in Fig. 1(b). The electric circuit is made mainly by three 20-m-long parallel conductors, 1.2 m apart, and connected in such a way that the current flowing in the central conductor is split in half in each of the outer ones. Direct currents from 0 kA to 2.5 kA, set with an uncertainty lower than 1 A, were injected in the central conductor. Given the distance between conductors and the maximum current intensity, mutual magnetic effects among parallel conductors are negligible. A loose tube containing standard G.652 optical fibers is helically wound on the conductors along the path ABCD [see Fig. 1(b)]. On conductors No. 1 and 3 the winding is right-handed (with respect to the ABCD direction) with radius $R \simeq 45$ mm and pitch $p \simeq 0.1$ m (correspondingly $\ell \simeq 0.3$ m). For completeness we report also that on conductor No. 2 the winding is left-handed with the same pitch and radius 25 mm; however this section will not be considered further being too short to be reliably analyzed. The total length of the wound loose tube is about 130 m. As an example the magnetic induction generated by 1 kA flowing in conductor No. 1 is about 4.4 mT at a radial distance $R \simeq 45$ mm, and the corresponding Faraday rotation per unit length of fiber at 1550 nm is as low as $\eta \simeq 5$ mrad/m.

One of the critical parameter in distributed polarization measurements is the spatial resolution δ_z, which should be set so to correctly sample $\hat{s}_B(z)$ [19]. Of course, the spatial variation of this SOP depends on both Faraday rotation and reciprocal birefringence. Actually, the latter is usually the dominant contribution, so the requirements on the measurement setup are in general imposed by the birefringence of the fiber, and not by the Faraday rotation we aim at measuring. In particular in the case at hand an important deterministic contribution to the reciprocal birefringence of the fiber comes from the helical winding [20–22]. The deterministic nature of this effect is clearly visible in the power spectral density (PSD) of the backscattered SOP, shown in Fig. 2(a). The curve refers to data measured at 0 A with spatial resolution of 5 cm, and represents the average of the normalized Welch's periodograms [23] of each component of $\hat{s}_B(z)$. It can be shown that the marked peak at about 2 m^{-1} is just a consequence of the ordered helical winding of the fiber. Specifically, bending, tension coiling and torsion all contribute to originate that peak [20–22]. In particular, bending and tension coiling give raise to a constant birefringence vector [20], whereas the torsion (which for the geometry at hand is about 7 rad/m) induces an apparent constant rotation of that vector [21, 22]. The result of these actions is a deterministic oscillation of the backscattered SOP, which manifests itself as a peak

#232204 - $15.00 USD Received 14 Jan 2015; revised 10 Mar 2015; accepted 12 Mar 2015; published 21 Apr 2015

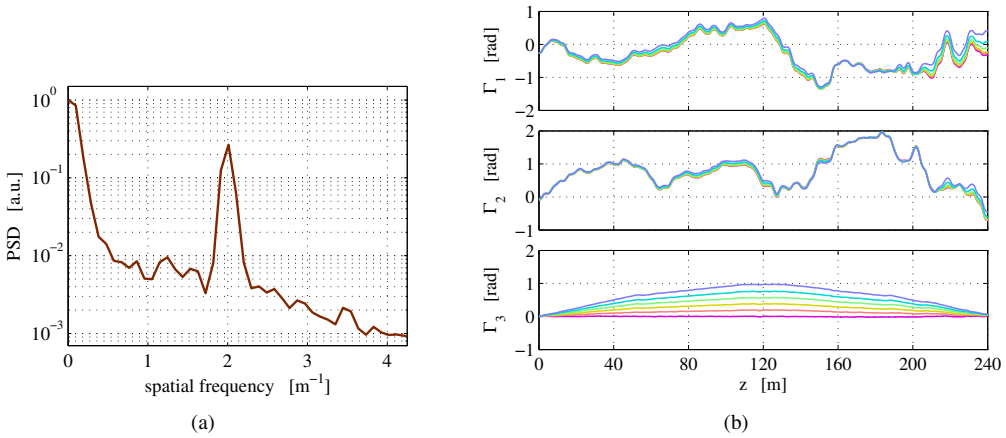

Fig. 2. (a) Power spectral density of the components of $\hat{s}_B(z)$. (b) Components of $\bar{\Gamma}(z)$ for different current intensities. With respect to the graph of Γ_3, curves (and respective colors) correspond (from the lower to the upper) to currents from 0 kA to 2.5 kA in steps of 0.5 kA.

in the PSD. Because of that peak the spatial resolution should in principle be lower than 25 cm, a value that in practical situations can hardly be guaranteed over long distances. Nonetheless, since in this case the winding effect is spectrally well separated from the base-band component of the spectrum (due to other intrinsic birefringence sources, including Faraday rotation), we can safely use a longer spatial resolution and enhance the measure SNR; this is basically equivalent to applying a low-pass filter to $\hat{s}_B(z)$. Of course, after filtering the backscattered SOP the information about linear birefringence is lost, but this is not of interest here. Differently, information about Faraday rotation is retained, since it appears in the base-band component of the spectrum. It is worthwhile stressing that the mathematical legitimacy of this filtering is in general not so trivial. Actually, while Faraday rotation and reciprocal birefringence are well separated in the birefringence vector $\bar{\beta}(z)$, they end up being highly entangled in $\hat{s}_B(z)$ by the nonlinear transformations that lead to the backscattered SOP [9]. Therefore, filtering $\hat{s}_B(z)$ is not equivalent to filtering $\bar{\beta}(z)$, and a filter applied on $\hat{s}_B(z)$ may in general result in a strong distortion of the calculated birefringence vector $\bar{\beta}(z)$.

Owing to the above argument, the components of the backscattered SOP have been filtered with a Gaussian filter, whose impulse response has a FWHM of 2.4 m, corresponding to a spatial resolution of about 1.2 m (i.e. 4 fiber loops). Measurements have been performed along 2 fibers of the loose tube concatenated at position D [see Fig. 1(b)]. Figure 2(b) shows the cumulative integrals $\bar{\Gamma}(z) = \int_0^z \bar{\beta}(u)\,du$, calculated using the values of $\bar{\beta}(z)$ measured for 6 different current intensities, varying from 0 kA to 2.5 kA in steps of 0.5 kA. The reason why we report the integral $\bar{\Gamma}(z)$ is to highlight the effects of Faraday rotation. We clearly see that the first two components of $\bar{\Gamma}(z)$ are independent of the current intensity as expected, and the corresponding 6 curves are overlapped, except for some residual noise. Differently the third component of $\bar{\Gamma}(z)$, i.e. the Faraday rotation accumulated along the link, has a marked dependence on the current flowing in the conductors.

The same data are more clearly represented in Fig. 3, where the different parts of the electrical circuit are highlighted. We see that along the first fiber on the first conductor (AB) the accumulated Faraday rotation increases linearly at a rate proportional to the current intensity. The same happens along the second conductor (CD), but here the slope is halved just because the current in CD is half of that in AB. At a distance of about 120 m the first fiber is connected

#232204 - $15.00 USD Received 14 Jan 2015; revised 10 Mar 2015; accepted 12 Mar 2015; published 21 Apr 2015

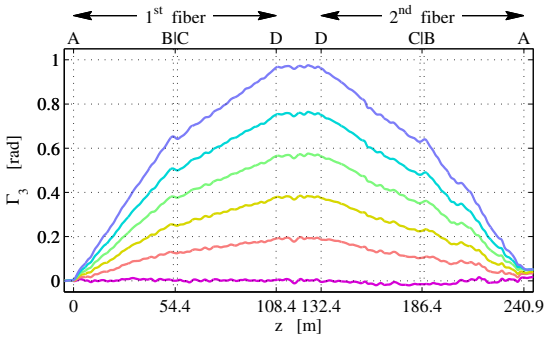

Fig. 3. Accumulated Faraday rotation for different current intensities (data, colors and conditions as in Fig. 2(b)). The top horizontal axis indicates positions with respect to the layout in Fig. 1(b).

to the second one, which after few meters enters again the loose tube and follows the ABCD path backward. Since in the second fiber the direction of forward propagation of light is flipped, the cosine in (1) changes sign and the Faraday rotation accumulated along the first fiber is unwound along the second one. Of course the slopes along conductors AB and CD are the same of the first fiber, but opposite in sign. A small change in the slope sign can be noted also along the sections between points B and C, which correspond to the short fiber sections around conductor No. 2 that are wound in opposite direction.

Since the current is constant in each conductor, a more quantitative analysis of the data in Fig. 3 can be obtained by interpolating the Faraday rotation accumulated along each conductor with a linear polynomial. Actually, considering a fiber section between z_0 and $z_0+\Delta z$, wound around the same conductor, the accumulated Faraday rotation reads ($z \in [z_0; z_0+\Delta z]$)

$$\Gamma_3(z) = \Gamma_3(z_0) + 2\mu_0 V I (z/\ell), \tag{2}$$

so by calculating the slope of this curve we determine the current I. In this respect Δz represents the ultimate spatial resolution (in terms of fiber length) with which the current is measured; similarly, $\Delta z_e = (p/\ell)\Delta z$ is the same resolution expressed in length of electric cable. The statistical properties of I can be estimated for every spatial resolution Δz by varying z_0 along the section at constant current. This ensemble of data can then be used to estimate the mean $\langle I \rangle$ and standard deviation σ_I of the estimate for each spatial resolution Δz. Figure 4(a) shows $\langle I \rangle$ measured over conductors No. 1 and 3. In both cases the dashed lines indicate the nominal current values and we see that there is a good agreement between these values and the measured ones, independently of the spatial resolution Δz. Differently, Δz has an impact on the standard deviation σ_I, as shown in Fig. 4(b). The values reported in the graph are the maximum standard deviations obtained for each Δz as the current and the analyzed conductor were varied; we report only one curve because σ_I is largely independent of the mean current value. Recalling that the winding pitch is 0.1 m, we see that the uncertainty is about 100 A with a spatial resolution Δz_e of about 4 m of electric cable, and can be reduced to about 30 A by increasing the spatial resolution to $\Delta z_e \simeq 10$ m. This improvement of the accuracy is mainly due to the increased length of the fiber over which the Faraday rotation is measured. As reported above, the magnetic field generated by 1 kA at the cable surface (i.e. at a distance $R \simeq 45$ mm) induces a Faraday rotation as low as 5 mrad/m. However, along 4 m of electric cable, which correspond to about 12 m of optical fiber, this amounts to a rotation of 60 mrad of the SOP. Correspondingly, the backscattered SOP experiences a rotation double than that, 120 mrad, which is large enough to be accurately measured, also thanks to the increase in the SNR due to the spatial filtering.

#232204 - $15.00 USD Received 14 Jan 2015; revised 10 Mar 2015; accepted 12 Mar 2015; published 21 Apr 2015

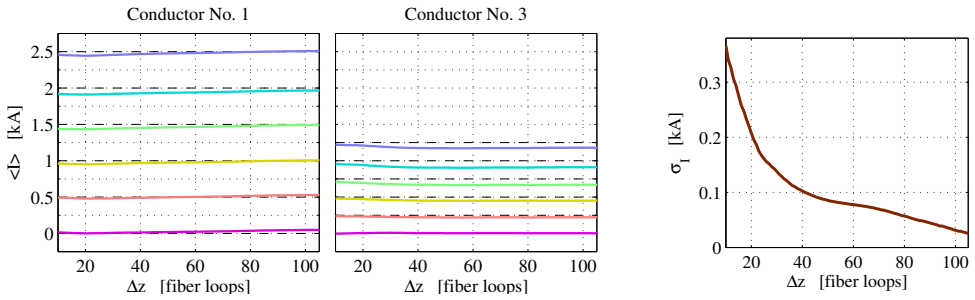

Fig. 4. (a) Mean values of the estimated current for different spatial resolutions; dashed lines are the nominal values (graphs share the same vertical axis). (b) Standard deviations of the estimated mean currents.

Despite the achieved sensitivity and distance range need to be further increased before the method could find application in the field, the results reported here confirm the viability of the proposed technique to distributedly monitor intense direct current along electrical cables. While tests have been performed on an equivalent electrical cable length of about 80 m, the successful use of spatial resolutions in the order of meters makes this technique compatible with time domain reflectometry, thus potentially appropriate to longer distance ranges.

Acknowledgment

This work has been supported by Prysmian S.p.A., Italy, within the project “Measurements of the evolution of the magnetic field in power lines by means of fiber-optic polarization-sensitive reflectometry.” A. G. acknowledges support from “High-end Foreign Expert Project”.

#232204 - $15.00 USD Received 14 Jan 2015; revised 10 Mar 2015; accepted 12 Mar 2015; published 21 Apr 2015